

Microstructure from joint analysis of experimental data and *ab initio* interactions: Hydrogenated amorphous silicon

Parthapratim Biswas,^{1,2,a)} D. A. Drabold,^{2,b)} and Raymond Atta-Fynn^{3,c)}

¹*Department of Physics and Astronomy, The University of Southern Mississippi, Hattiesburg, MS 39406, USA*

²*Department of Physics and Astronomy, Condensed Matter and Surface Science Program, Ohio University, Ohio 45701, USA*

³*Department of Physics, The University of Texas, Arlington, Texas 76019, USA*

(Received 9 September 2014; accepted 13 December 2014; published online 29 December 2014)

A study of the formation of voids and molecular hydrogen in hydrogenated amorphous silicon is presented based upon a hybrid approach that involves inversion of experimental nuclear magnetic resonance data in conjunction with *ab initio* total-energy relaxations in an augmented solution space. The novelty of this approach is that the voids and molecular hydrogen appear naturally in the model networks unlike conventional approaches, where voids are created artificially by removing silicon atoms from the networks. Two representative models with 16 and 18 at. % of hydrogen are studied in this work. The result shows that the microstructure of the a-Si:H network consists of several microvoids and few molecular hydrogen for concentration above 15 at. % H. The microvoids are highly irregular in shape and size, and have a linear dimension of 5–7 Å. The internal surface of a microvoid is found to be decorated with 4–9 hydrogen atoms in the form of monohydride Si–H configurations as observed in nuclear magnetic resonance experiments. The microstructure consists of (0.9–1.4)% hydrogen molecules of total hydrogen in the networks. These observations are consistent with the outcome of infrared spectroscopy, nuclear magnetic resonance, and calorimetry experiments. © 2014 AIP Publishing LLC. [<http://dx.doi.org/10.1063/1.4905024>]

I. INTRODUCTION

Hydrogenated amorphous silicon (a-Si:H) is one of the most important electronic materials, having applications in solar cells,^{1,2} night-vision devices,³ thin-film transistors,⁴ position-detection sensors,⁵ liquid crystal display,⁶ and many other electro-optical devices.^{7–9} Since the “dangling bond” defect density is very high in pure amorphous silicon (a-Si), it is necessary for electronic applications to passivate these defects with hydrogen. Addition of hydrogen, however, not only changes the electronic properties but also introduces structural changes at the microscopic level. In small doses, it is expected that H primarily ameliorates defects by passivating sp^3 dangling bonds. At the higher concentrations actually employed in most devices however, it also can act as an “etching agent” and break linkages between Si atoms and stimulate the production of voids. Furthermore, the hopping of H is important at higher temperatures,¹⁰ and this hopping must also have an effect on network connectivity.

H-induced microstructural changes produce strong inhomogeneities on the nanometer length scale. Such structures play a major role in determining the properties of a-Si:H.^{11,12} For example, neutron scattering data suggest that the microstructural changes associated with light irradiation can affect the network structure up to several nanometers.¹³ This has implications in understanding Staebler-Wronski effect (SWE)¹⁴—a light-induced degradation of the optical properties of a-Si:H. Since hydrogen can alter the network

structure of a-Si, the inclusion of too much hydrogen can be detrimental to its electronic properties as well. Amorphous silicon films containing 7–15 at. % of hydrogen are generally considered as device quality, and correspond to defect density of about 10^{15} defects/cm³. While the role of “dangling bonds” defects has been studied extensively in the literature,^{7,8} defects associated with inhomogeneities at the nanometer length scale, e.g., voids, poly-vacancies, and columnar growth, are less understood and studied. This statement particularly applies to the theoretical studies of voids and molecular hydrogen in hydrogenated amorphous silicon. Despite the availability of an array of excellent experimental data from neutron^{15–17} and X-ray scattering,^{13,18–20} nuclear magnetic resonance (NMR),^{21–25} and infrared (IR) absorption measurements,^{26–30} there are few theoretical studies that directly address the nature of these strong inhomogeneities present in the network and their roles in the electronic and optical properties of a-Si:H.

The purpose of this paper is to present the results from a recent study that addresses voids and molecular hydrogen in hydrogenated amorphous silicon at high concentration. The study demonstrates that a recently developed hybrid approach³¹ that merges experimental data and a first-principles total-energy functional simultaneously in an augmented solution space has the ability to produce configurations of a-Si:H, where voids and molecular hydrogen appear naturally during hydrogenation of the network. The approach essentially consists of generating a real-space distribution of H atoms via the inversion of experimental NMR data within the solution space constrained by an appropriate total-energy functional in a self-consistent manner, and provides direct evidence of the

^{a)}Electronic address: Partha.Biswas@usm.edu

^{b)}Electronic address: drabold@ohio.edu

^{c)}Electronic address: attafynn@uta.edu

formation of voids in models of hydrogenated amorphous silicon. We emphasize that this approach is unbiased: both the dimension and the very existence of the voids are derived from experimental data, while using *ab initio* interactions to ensure that the configurations obtained are energetically and electronically valid. This is in contrast to earlier work, wherein voids were introduced artificially for studying their effects on the model *a*-Si:H networks and the dynamics of hydrogen atoms. The present study shows that structural configurations obtained via the hybrid approach not only satisfy experimental input data but also the structural, electronic, and other microstructural properties of *a*-Si:H. The formation of voids has been observed to depend, among other factors, on the amount of hydrogen present in the network and can be influenced by changing the concentration of hydrogen. The study also indicates that hydrogen molecules can appear inside the voids. The shape and the size of the voids, and the bonding environment of the hydrogen atoms near the void boundary, are also addressed in this study.

Where NMR is concerned, the rigid-lattice spectrum can be obtained by a full diagonalization of the secular dipolar Hamiltonian, from which the spin-correlation functions are easily constructed.³² This approach yields a 2^n -dimensional spin Hamiltonian, for n the number of spins, and worse, the matrix is dense because of the power-law (r^{-3}) fall off of the dipolar interaction. In a celebrated paper,³³ Van Vleck showed that it was easy to compute the power moments of the spectral density (Fourier Transforms) of the free induction decay (FID). Alternately, one can view these moments as Taylor coefficients of the FID. The moment method makes an implicit assumption that the spins are all well coupled (assuming a rough equivalence in the spin-spin interactions from site to site). In the language of NMR, one would call this a homogeneously broadened line. While our system is most certainly *not* spatially homogeneous, it probably is *spectrally* based upon a detailed study that suggests that a spin concentration of 10% is enough to ensure homogeneous broadening. For lower concentrations of H (outside the scope of this paper), this assumption is probably invalid.

The rest of the paper is organized as follows. Section II summarizes the results from the literature. In Sec. III, a brief description of the hybrid approach for generating hydrogen distributions is presented. Section IV focuses on the validation of these models by addressing the total pair-correlation functions, the bond-angle distribution, and the electronic density of states. An analysis of the hydrogen distribution in real space with an emphasis on the nature of various silicon-hydrogen bonding configurations is also included here. The results for the voids and molecular hydrogen are presented in Sec. V, which is followed by a conclusion in Sec. VI.

II. EARLIER WORKS: AN OVERVIEW

Over the past decades, there has been a number of experimental studies that have addressed structural properties of *a*-Si:H via X-ray^{15–17} and neutron diffractions,^{13,18–20} nuclear magnetic resonance,^{23–25,34} electron microscopy,³⁵ infrared spectroscopy,^{26–29} and calorimetry experiments.^{20,36,37} Results from earlier studies on hydrogenated amorphous

silicon were reviewed by Elliott,³⁸ Knights,³⁹ and Taylor.⁴⁰ While these studies have provided a wealth of information on various microstructural properties of the material, the exact character of the voids and their role in the dynamics of hydrogen diffusion in the amorphous environment is still not fully understood, and is a subject of continued interest. Small angle X-ray scattering (SAXS) is particularly useful in providing quantitative information about the shape, size, and number density of the inhomogeneities by detecting the fluctuations associated with the electron density in the inhomogeneous regions. A characterization of microvoids in a device-quality glow discharge sample of *a*-Si:H was made by Mahan *et al.*^{41,42} by combining SAXS with IR measurements. Their observation suggests that within the Guinier approximation⁴³ in which the inhomogeneities are dispersed in a homogeneous medium, the radius of the microvoids lies between 6.0 Å and 12.0 Å, and that the interior surfaces of the microvoids are decorated with approximately 4–9 hydrogen atoms bonded to the silicon atoms on the void boundary. In the experiment of D'Antonio and Konnert¹⁵ on glow discharge samples with 15 at. % hydrogen, the distribution of void volumes was extracted from SAXS data, and it was found that the radius of gyration of the voids mostly corresponded to 6–16 Å. Since hydrogen is a strong neutron scatterer, use of neutrons instead of X-ray can provide information on the real-space pair correlation function (PCF) in the wide-angle scattering and the average size of the inhomogeneous regions (e.g., hydrogen clusters) in the small-angle neutron scattering limit (SANS). Neutron scattering has a unique advantage over X-ray; for example, by isotopic substitution of hydrogen with deuterium, it is possible to extract information about the various partial pair-correlation functions of the constituent atoms. Postol and co-workers,¹⁸ and Bellissent *et al.*^{13,44} obtained the partial pair-correlation functions for sputtered *a*-Si:H samples with 14 and 16 at. % hydrogen, respectively. Small-angle neutron scattering data obtained in their studies were indicative of the presence of large inhomogeneous structure with a linear dimension of 270 Å and 125 Å, respectively. Recently, Wright *et al.*¹⁹ have performed a high-resolution neutron diffraction study on hydrogenated and deuterated samples of glow discharge amorphous silicon, and have reported the presence of voids with a Guinier radius of 5–6 Å. These results are consistent with the outcome of NMR experiments.^{22–25} Multiple-quantum nuclear magnetic resonance (MQ-NMR)²³ data conclusively demonstrate the presence of large hydrogen clusters, particularly at high concentration (≥ 15 at. %) of hydrogen. The cluster size estimated from NMR data is consistent with the size of the inhomogeneities observed in SAXS and SANS studies. Infrared spectroscopy studies by Smets *et al.*⁴⁵ also provide evidence for the existence of microvoids above 14 at. % hydrogen. The discovery of occluded/trapped molecular hydrogen inside the voids at high pressure is further indicative of the presence of voids in *a*-Si:H. This presence of molecular hydrogen in *a*-Si:H was first proposed by Conradi and Norberg³⁶ to explain the anomalous temperature dependence of hydrogen NMR spin-lattice relaxation time observed by Carlos and Taylor.³⁴ Thereafter, a series of additional NMR,^{22,25} calorimetry,^{20,37} and infrared absorption measurements^{46,47} confirmed the presence of approximately (0.5–1) at. % H₂ in *a*-Si:H. The

signature of molecular hydrogen also manifests in the NMR spectrum in the form of a powder-averaged Pake doublet⁴⁸ at low temperature. Boyce and Stutzmann⁴⁹ have observed such a doublet with a line-splitting of 175 kHz in plasma-deposited *a*-Si:H samples. These authors have noted a four-fold increase in the molecular hydrogen concentration, from 0.25 at. % in as-deposited films to 1 at. %, upon annealing. While the accuracy of these studies vary among themselves, these studies suggest that voids and molecular hydrogen are present in *a*-Si:H with the exact size and the number of H molecules being depend upon the concentration of hydrogen, growth conditions, and sample treatment.

Theoretical studies on voids are few and far between. While there exist a variety of theoretical studies on homogeneous systems^{50–53}—from empirical and tight-binding to *ab initio* approaches—that focus on the structural, electronic, and vibrational properties of hydrogenated amorphous silicon, few of these address the presence of voids and molecular hydrogen. The difficulty associated with hydrogenating a large amorphous silicon network, that is necessary for the inhomogeneities to materialize in the nanometer length scale, continues to be a major obstacle in *ab initio* studies of voids. The few studies that do address the issue are based on the assumption that voids exist in amorphous silicon, and then proceed to create these voids artificially by removing silicon atoms from previously built models of amorphous silicon. Earlier studies include the effect of voids on the structure factor of amorphous silicon.⁵⁴ The study shows that the presence of voids increases the structure factor at very small wave vector below 1.0 \AA^{-1} as observed in the small-angle scattering experiments on *a*-Si (Ref. 15) and *a*-Si:H.¹³ Drabold and co-workers have studied the dynamics of hydrogen atoms within the voids,^{55,56} and the effect on the vibrational density of states⁵⁷ via *ab initio* molecular dynamics (AIMD) simulations. While these studies do reveal some useful information on the dynamics of H atoms in the presence of voids, direct evidence for the presence of voids cannot be inferred from such studies. Thus information on the shape and the size of the voids, their distributions, and the correlation between the size and the concentration of hydrogen present in the network cannot be obtained from these works. A fundamental question here is the mechanism of void formation in an amorphous network and, to what extent, the presence of hydrogen atoms can affect such a mechanism. To address some of these questions, it is necessary to generate large models of *a*-Si:H via an approach that is capable of forming voids naturally as the (hydrogen) microstructure of a network evolves during hydrogenation.

III. INFORMATION-BASED PARADIGM FOR STRUCTURAL INVERSION, GUIDED BY *AB INITIO* INTERACTIONS

The hybrid strategy employed here to generate a hydrogen distribution relies on the inversion of experimental nuclear magnetic resonance data.³¹ Since the structure of amorphous silicon can be obtained by a variety of methods,^{58–60} the key problem involves incorporating a correct distribution of hydrogen in a model of amorphous silicon. In

the conventional approach, the problem is addressed by passivating the dangling bonds with hydrogen, which is followed by a relaxation of the new configuration via a first-principles total-energy functional. While such an approach can produce a reasonably good model,^{50,51,61,62} the final hydrogen distribution obtained in this approach is constrained by, and correlated to, the distribution of dangling bonds in the starting amorphous silicon network, and subject to the *a priori* biases of the modeler.

The hybrid approach specified here is based upon the assumption that by inverting one-dimensional NMR spectra, it is possible to construct model three-dimensional distribution of hydrogen atoms in real space. Such inversions cannot be achieved uniquely for a given NMR spectrum alone and, thus, necessitates the use of additional information, such as the size of hydrogen clusters derived from experimental NMR data, and critically, accurate total energies and forces from a current *ab initio* code. A detailed description of the approach and its implementation can be found in Ref. 31. Hereafter, only the key steps of this approach are outlined.

First, an ensemble of hydrogen distributions is constructed that takes into account the presence of hydrogen clusters and their sizes as obtained from NMR experiments.^{22–24} Apart from the presence of few clusters, hydrogen atoms are randomly distributed in a box for a given density and concentration. Second, the first two non vanishing Van Vleck moments (μ_2, μ_4)³³ of the NMR spectrum are calculated from the proton positions, and are matched to the moments obtained from the experimental NMR spectra. Together with the cluster data, these NMR *optimized* prior distributions represent the possible solutions for a hydrogen distribution. Third, the optimized hydrogen distributions are merged with a previously built amorphous silicon network. In the present study, an amorphous silicon network of about 2500 atoms enclosed in a cubic box of size 35.7 \AA has been used as a background amorphous matrix. In the process of merging an optimized hydrogen distribution with a silicon matrix, silicon atoms that overlap with the hydrogen atoms at a distance less than the silicon-hydrogen bond length ($1.4\text{--}1.5 \text{ \AA}$) are removed. None of the hydrogen atoms is removed to preserve the experimental cluster and moment information. Finally, the combined silicon-hydrogen network is relaxed using the first-principles density functional code SIESTA.⁶³ A schematic diagram showing the various steps of the method is included in the supplementary materials.⁶⁸

The total-energy calculation is done using the first-principle density-functional code SIESTA. The Perdew-Zunger formulation of the local density approximation (LDA)⁶⁴ is employed in this work along with the norm-conserving Troullier-Martins pseudopotentials,⁶⁵ which is factorized into the Kleinmann-Bylander form.⁶⁶ SIESTA employs pseudoatomic orbital basis sets to describe the valence electrons that consist of the finite-range numerical pseudoatomic wave functions as proposed by Sankey and Niklewski.⁶⁷ In the present work, a minimal or single- ζ basis is used for Si atoms, whereas a double- ζ basis is chosen for H atoms.⁶³ The system is thoroughly relaxed by solving the Kohn-Sham equations using the full self-consistent field approach to obtain the final structure. While the approach can be

employed to generate a hydrogen configuration in a range of concentrations, for the purpose of studying voids and molecular hydrogen, we focus on two model configurations with 16 and 18 at. % of hydrogen. Hereafter, the models are referred to as models A and B, respectively.

IV. MODEL CHARACTERIZATION: STRUCTURAL AND ELECTRONIC PROPERTIES

Before addressing the microstructural properties of the networks, we briefly examine the two- and the three-body correlation functions for models A and B, and compare the results to diffraction experiments. A preliminary analysis of the structure can be obtained by studying the total radial distribution function (RDF). It should be noted that while a two-body correlation function is not sufficient to characterize a three-dimensional structure uniquely, it is necessary for any computer-generated model to have the correct radial distribution function that matches the experimental data.⁶⁸ In addition to the RDF, the bond-angle distribution and the coordination number of the atoms are examined to determine the structural properties of the models that cannot be obtained via the two-body correlation function.⁶⁹ In the following, the neutron-weighted total correlation function is computed in real space, and is compared directly to the experimental data available in the literature. Assuming $\rho_{ij}(r)$ be the average number density of j th atoms at a distance r from the i th atoms, the partial pair-correlation function $g_{ij}(r)$ can be expressed as the ratio of the density $\rho_{ij}(r)$ to the homogeneous density ρ_j of j th atoms³⁸

$$g_{ij}(r) = \frac{\rho_{ij}(r)}{\rho_j} = \frac{\rho_{ij}(r)}{c_j \rho_0}.$$

Here, c_j is the atomic fraction of the j th species and $\rho_j = c_j N/V = c_j \rho_0$. The total radial distribution function $J(r)$ can be written as

$$J(r) = 4\pi r^2 \rho_0 \sum_{i,j} A_{ij} g_{ij}.$$

The weighting factors A_{ij} are given by

$$A_{ij} = \frac{c_i c_j b_i b_j}{b_{avg}^2}, \quad b_{avg} = \sum_i c_i b_i,$$

where c_i and b_i are the atomic fraction and the neutron scattering factor for the i th species, respectively. For the purpose of comparison to the experimental data in Ref. 19, the correlation function $T(r) = J(r)/r$ is computed here.

The total correlation function $T(r)$ for model B is plotted in Fig. 1 along with the experimental data from Ref. 19. The results match the experimental data very well considering the fact that model B corresponds to 18 at. % H, whereas the experimental data are for 22 at. %H. The first dip in the data near 1.5 Å in Fig. 1 corresponds to Si–H bond length, and the negative value results from the neutron scattering factor of H atoms. The apparent deviation of the theoretical result from the experimental data near 1.5 Å can be attributed to the difference of hydrogen concentration, which results in a

less number of Si–H bonds in model B. The average bond angles for models A and B are found to be 108.65° and 108.55° with a corresponding root mean square deviation of approximately 13.4° and 13.1°, respectively. Further characterization of the models is possible by calculating the coordination numbers of the silicon atoms and the electronic density of states. For model A, approximately 98.4% of silicon atoms are found to be four-fold coordinated, whereas 0.9% and 0.6% of Si atoms have a coordination number 5 and 3, respectively. This translates into an averaged coordination number of 3.99. The corresponding numbers for model B are 97.7%, 1.5%, 0.8%, and 4.004, respectively. The electronic density of states (EDOS) for the models is calculated within the LDA via SIESTA to examine the effects of few under- and over-coordinated atoms on the EDOS, particularly near the bandgap region. Figure 2 shows the EDOS for models A and B. Although the size of the gap is underestimated in both the cases,⁷⁰ it is reasonably clean and consistent with the use of the LDA, and the overall shape of the EDOS matches the experimental data^{7,38} and the theoretical results obtained by others.^{52,77}

Having discussed the structural and electronic properties of the hybrid models, we now briefly address the nature of hydrogen microstructure in the networks. Experimental data from NMR and IR spectroscopy indicate that the microstructure of hydrogen in α -Si can be highly inhomogeneous depending on the method of preparation, growth conditions, and the concentration of hydrogen in the samples. Nuclear magnetic resonance experiments suggest that the microstructure (of H) typically consists of clustered and sparse distribution of H atoms, whereas infrared spectroscopy indicates the presence of various silicon-hydrogen bonding configurations by measuring the vibrational frequencies of the bonded hydrogen atoms. A real-space analysis of models A and B does confirm this observation. The hydrogen microstructure is found to be highly inhomogeneous with a variety of several silicon-hydrogen bonding configurations that are realized in a clustered and a sparse environment (of H atoms).

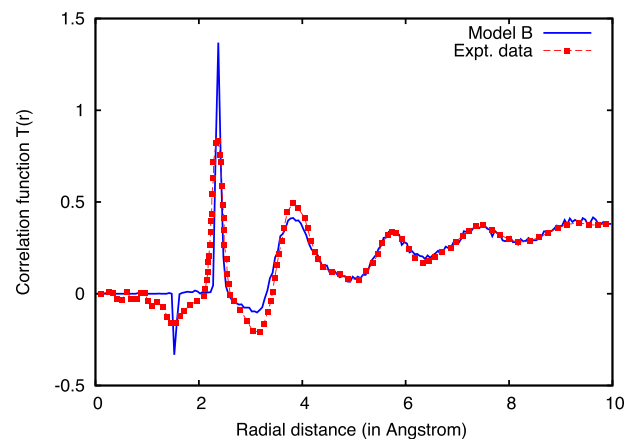


FIG. 1. Neutron-weighted total correlation function $T(r)$ for model B as a function of the radial distance. Experimental data (°) correspond to 22 at. % of hydrogen and are reproduced by permission from A. C. Wright *et al.* J. Phys.: Condens. Matter **19**, 415109 (2007). Copyright 2007 by IOP Publishing.

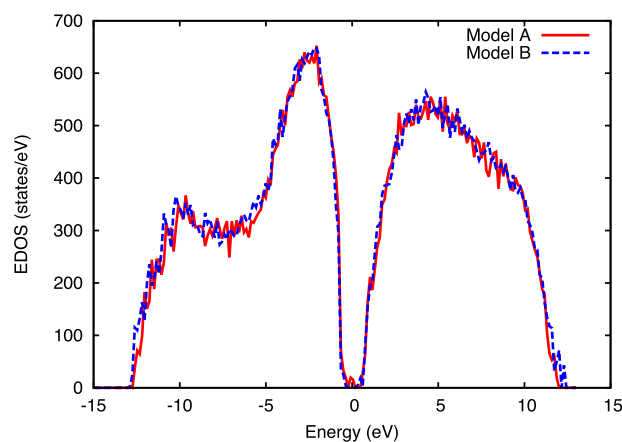


FIG. 2. The density of electronic states for models A (16 at. % H) and B (18 at. % H) as a function of energy. The Fermi level is located at $E_f = 0.0$ eV.

The distribution of hydrogen is mostly dominated by mono- and dihydride configurations, which is in agreement with IR experiments^{26–29} as well as with the results obtained from the recent theoretical works on hydrogen microstructure.^{71,72} Analysis of various hydrogen-bonding configurations in model A shows that approximately 74.6% of total hydrogen atoms are bonded to silicon as SiH, 21.1% as SiH₂, 2.9% as SiH₃, and only 1.4% as molecular hydrogen (H₂). The corresponding numbers for model B are 75.4% (SiH), 19.6% (SiH₂), 3.3% (SiH₃), and 0.9% (H₂). The statistics of various silicon-hydrogen bonding configurations along with the percentage of hydrogen atoms in clustered and dilute phases are listed in Table I. The majority of the H atoms are found to be realized in a clustered phase, as is expected at high hydrogen concentration. Likewise, there are a few H atoms that appear as a part of a very dilute phase, which are separated by at least 3.0 Å from the neighboring H atoms. The remaining H atoms are dispersed in an intermediate phase, which is neither a clustered nor dilute. The spatial inhomogeneity of the hydrogen distribution can be studied further by partitioning the entire network into several small non-overlapping regions, and analyzing the distribution of hydrogen atoms in these regions.

In Fig. 3, the results obtained by partitioning model A into a number of cubic cells of linear dimension 7.0 Å are presented. The average number of H atoms in a cell is indicated in Fig. 3. This average depends on the size of the cell and, for a cell of size 7.0 Å, is given by $N_H = 3.3$. Although, this one-dimensional plot does not provide a full picture of the real-space distribution of hydrogen atoms in the network, the fluctuation in the number of atoms in different cells does indicate a high degree of inhomogeneity in the real-space distribution of hydrogen atoms. For example, it is evident from Fig. 3, there are seven hydrogen-rich regions in the network that have more than eight hydrogen

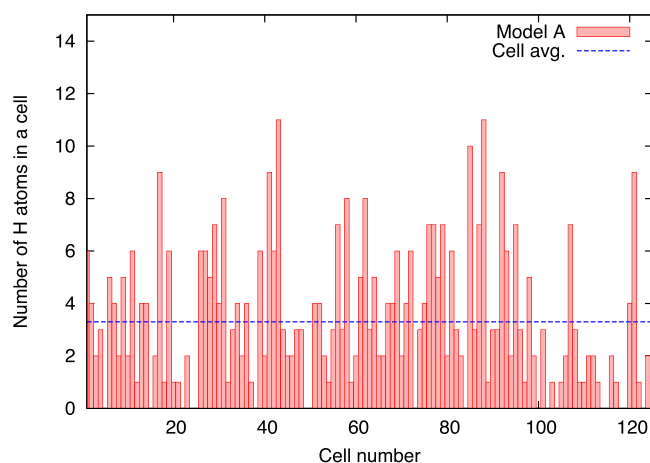


FIG. 3. The distribution of hydrogen in model A via partitioning the network into non-overlapping cells. The inhomogeneity in the microstructure is reflected in the number of H atoms within the cells. The average number of H atoms in a cell is indicated as a horizontal line.

atoms for a partition size of 7.0 Å. Similarly, there are several regions in the network that have few hydrogen atoms in the form of a monohydride or a dihydride configuration that indicates the presence of isolated Si–H and H–Si–H bonding. Such regions, when appear next to each other, can form a sparse or a dilute distribution of H atoms, and have been observed in the NMR and the IR studies. Likewise, the absence of hydrogen atoms in several regions is also apparent from the histogram in Fig. 3. Although the exact number of H clusters depends to an extent on the size of the partition, a further analysis reveals that approximately (35–50)% of total H atoms reside in the clustered phase, including several small cluster of 4–7 H atoms and few large clusters of 8–13 H atoms having a linear dimension in the range 4.0–7.0 Å. An example of such a cluster from models A and B is shown in Figs. 4 and 5, respectively. The radius of both the silicon-hydrogen complexes in the figure is about 5.0 Å, and consists of 9 and 11 hydrogen atoms. The Gaussian isosurface⁷³ surrounding the silicon and hydrogen atoms is also drawn to indicate the void region inside the complexes.

V. VOIDS AND MOLECULAR HYDROGEN

Voids are nanoscale inhomogeneities that introduce density fluctuations in the network of amorphous silicon. The absence of several atoms in a network generally constitutes a microvoid and can have a radius of 5–20 Å depending on the number of missing atoms. Experimental data^{13,15,19,22,41} suggest that the presence of voids in hydrogenated amorphous silicon is strongly influenced by the method of preparation, growth conditions, and the concentration of hydrogen in a sample. Hydrogen evolution experiments via calorimetry

TABLE I. Hydrogen distribution in models A and B.

	Si–H (%)	SiH ₂ (%)	SiH ₃ (%)	H ₂ (%)	H in clustered phase (%)	H in dilute phase (%)
Model A	74.6	21.1	2.9	1.4	35–51	10–12
Model B	75.4	19.6	3.3	0.9	30–53	10–13

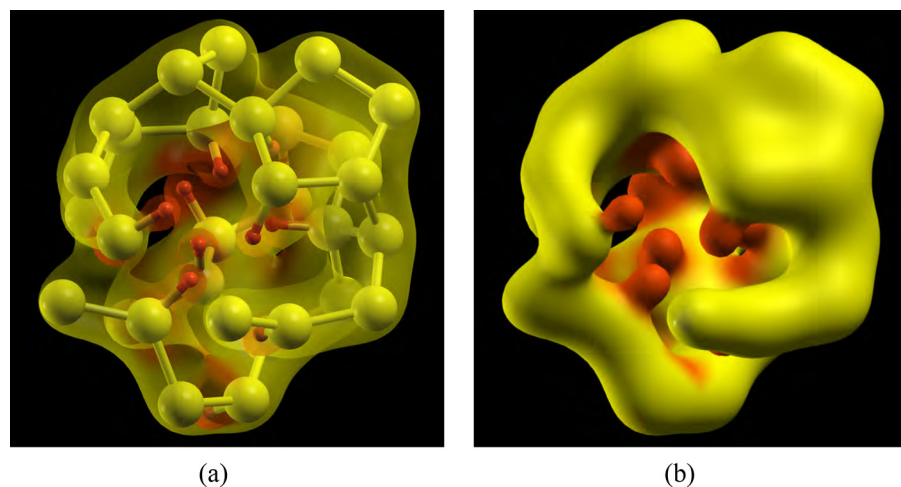


FIG. 4. (a) A hydrogen-rich region in model A showing nine hydrogen atoms (small/red) in a spherical complex of radius 5.0 Å. The Gaussian isosurfaces (transparent) are also indicated. (b) The same complex but with the Gaussian isosurface drawn around the hydrogen (small/red) and silicon (large/yellow) atoms.

indicate that amorphous Si:H films produced via radio frequency glow discharge method at low deposition temperature ($<150^{\circ}\text{C}$) tend to form an open, void-rich structure.²⁰ However, a more compact structure results at high substrate temperature ($>200^{\circ}\text{C}$) that makes it difficult for the trapped hydrogen to diffuse through the network. Although microvoids have been observed in device-quality a-Si:H samples, it is now generally accepted that the presence of voids is facilitated with increasing hydrogen concentration and can degrade the electronic quality of the samples at high concentration beyond 18–20 at. %H. SAXS data combined with infrared absorption experiments suggests that the surface of a microvoid is decorated with 4–9 hydrogen atoms bonded to the silicon atoms on the surface.⁷⁴ The discovery of occluded/trapped hydrogen at high pressure is further indicative of the presence of voids in hydrogen-rich a-Si networks.^{22,34,36,46,47}

Ab initio simulations of voids in a-Si:H are confronted with two major difficulties. First, since the voids are nanoscale inhomogeneities, a large model with a linear dimension of several tens of nanometer is needed from scratch for the voids to realize in the network. However, the cubic scaling of (computational demand) most *ab initio* algorithms with the system size makes it very difficult and computationally hard to generate such large realistic models of a-Si:H. Second, even if an improved scaling approach is available, there is no guarantee that the correct structure of

a-Si:H can be obtained from direct AIMD simulations. Since amorphous silicon is not a glass, the conventional “melt-quench” procedure via AIMD tends to produce poor a-Si:H networks with too many defects. While the problem can be ameliorated by employing amorphous silicon networks obtained from other approaches,^{58–60} the hydrogenation of the pure a-Si network continues to pose a problem. The majority of the current approaches follows the latter that involves passivation of the dangling bonds of a pure amorphous silicon network, and subsequent relaxation (or annealing) of the resulting configuration by using a first-principle total-energy functional. The process is then repeated until the defect density and the concentration of hydrogen are within an acceptable limit. A number of a-Si:H models have been produced following this route that correctly describe the structural, electronic, and the vibrational properties of a-Si:H.^{50–53,61,62} However, none of these models shows the presence of voids in the structure. The hallmark of the present hybrid approach is that the voids, vacancies, molecular hydrogen, and other characteristic features of hydrogen microstructure evolve naturally during hydrogenation of the network via the inversion of NMR moments in the augmented solution space. This remarkable feature distinguishes the hybrid approach from the conventional first-principle methods where the only recourse to study voids is to create them artificially in the networks.

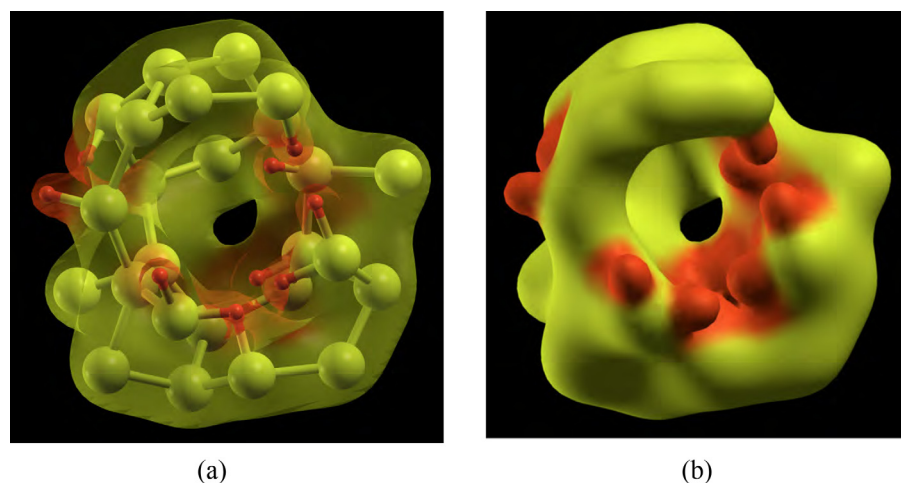


FIG. 5. (a) A hydrogen cluster in model B showing 10 hydrogen atoms (small/red) in a spherical complex of radius 5.0 Å. (b) The Gaussian isosurfaces (of the same complex) surrounding the hydrogen (small/red) and silicon (large/yellow) atoms are also shown.

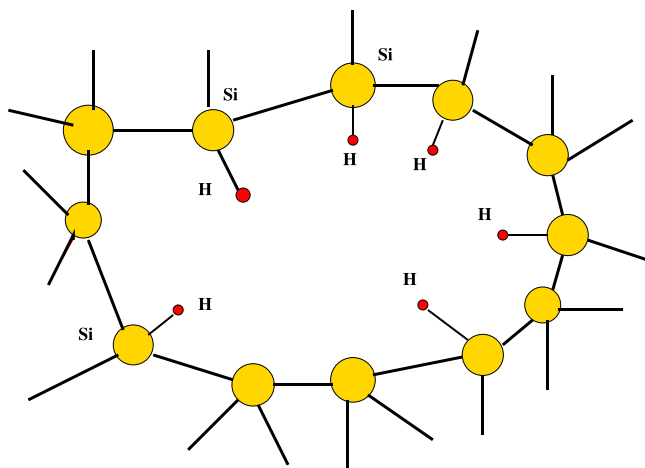


FIG. 6. A schematic representation of a void in a two-dimensional silicon complex. Hydrogen atoms (small/red) are bonded to the silicon atom (big/yellow) on the void surface. Such complexes in three-dimension have been realized in models A and B.

A real-space analysis of the hybrid models in the concentration range 10–22 at. %H reveals that the voids are more likely to form at concentrations above 15%. Although the current implementation of the method does not permit us to track the real-time dynamics of void formation, an examination of relaxation steps reveals that a void is likely to evolve during structural relaxation in the vicinity of a clustered hydrogen environment, a consequence of hydrogen “etching.” The presence of several hydrogen atoms in the form of mono- and dihydrides stimulates the formation of a void. The network reduces its strain during relaxation by rearranging the hydrogen and silicon atoms near the clustered hydrogen region, which in turn produces a void in the region. This possibly explains the presence of hydrogen atoms on the surface of a void.^{20,41} A schematic representation of such an arrangement (in two-dimension) is shown in Fig. 6. Due to the limited size of the models, the microvoids observed here are relatively small in size and have a diameter in the range of 5.0–7.0 Å. Figure 7 shows the structure of two microvoids that have been observed in models A and B. The radius of the silicon-hydrogen complexes shown in the figure is about 6.0 Å, and this includes a cavity of linear size 3.0–3.4 Å. The latter has been detected by partitioning the

entire model into a number of small cubic cells. The local density of the atoms associated with each cell is calculated to identify the low-density or void regions. For visual clarity, the Gaussian isosurfaces associated with the silicon and hydrogen atoms are also shown in Fig. 7 that indicate the regions with no atoms (i.e., voids). Figure 8 shows another representative void that realizes in model B with a number of monohydride configurations on the surface of the void. This can be understood as a three-dimensional analog of the two-dimensional (schematic) diagram shown in Fig. 6. Analysis of the void surface shows that nine monohydride (SiH) configurations have been realized on the surface of this void. The presence of such SiH configurations appears to be related to the concentration of H atoms in the networks. While few such SiH configurations have been observed at low concentration (model A) on the void surface (cf. left image in Fig. 7), the presence of more H atoms at high concentration facilitates the formation of SiH configurations near a void boundary as observed in Fig. 8.

Finally, it is important to note the presence of few molecular hydrogen that has been observed in the hybrid models based only upon inference from experiment and *ab initio* interactions. As mentioned in Sec. II, voids are intimately related to the presence of molecular hydrogen, particularly at low temperature and high pressure. Originally suggested from calorimetric measurements³⁶ and later confirmed by infrared and NMR experiments,^{22,46,47,75} it is now accepted that depending on the temperature, pressure, the method of preparation and the growth conditions, hydrogenated amorphous silicon may contain up to 1 at. % of molecular hydrogen.^{37,49} Owing to the static nature of the hybrid approach, the thermodynamics of molecular hydrogen cannot be addressed here unless an appropriate statistical ensemble is introduced to study the models further. Nonetheless, it is interesting to note that few molecular hydrogen have been realized in the static hybrid models. Analysis of models A and B shows the presence of few hydrogen molecules with a bonding distance less than 0.87 Å, which has been also reflected in the H–H pair-correlation function (see supplementary materials for details). At first glance, it may appear to be an artifact of incomplete relaxation of the network that might have caused two hydrogen atoms to come closer to form a molecule-like configuration. However, subsequent

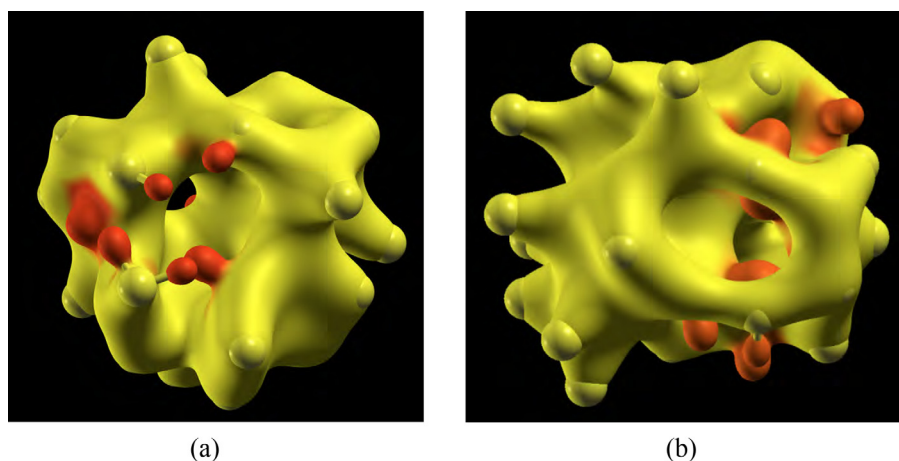


FIG. 7. (a) A Gaussian isosurface of a silicon-hydrogen complex of radius 6.0 Å showing the presence of a microvoid in model A. The radius of the void is between 3.5 Å and 3.75 Å. (b) A void of radius 3.7–3.8 Å realized in model B within a silicon-hydrogen complex of radius 6.0 Å. Silicon and hydrogen atoms are shown in yellow and red color, respectively.

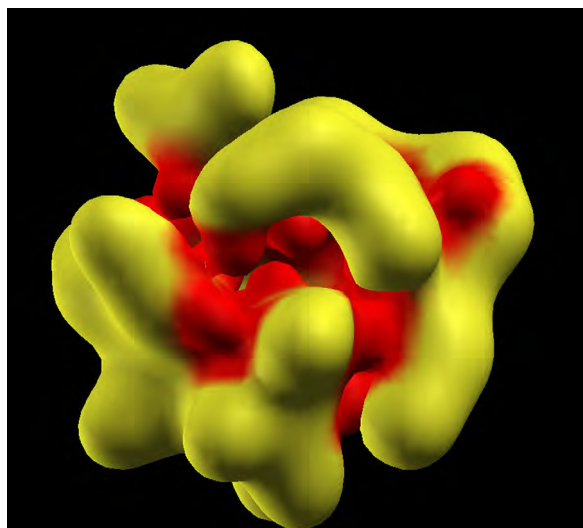


FIG. 8. A representative void structure (from model B) with several Si–H configurations on the surface of a void. The figure shows the Gaussian isosurface surrounding the silicon (yellow) and hydrogen (red) atoms. A low isovalue (i.e., more broadened) is used to highlight the “void” region inside the complex.

relaxations show that these H–H configurations are very stable under perturbation, and a further analysis of the local network reveals that the nearest silicon atom in all the cases is at a distance of more than 2.6 Å. The nearest hydrogen (in SiH) from these H–H configurations is found to be within a distance of 3.5–4.5 Å. Therefore, it is more likely that that these H–H configurations indeed represent hydrogen molecules that are realized within the microvoids. It may be noted that the spin-echo experiments coupled with T_1 measurements by Fry *et al.*⁷⁶ suggest that hydrogen molecules should be at least 10 Å away from the nearest atomic hydrogen. This assertion, however, was deduced for occluded H_2 at high pressure and low temperature. Thus, it is not unexpected to observe few H_2 molecules in a microvoid with a diameter of 5–7 Å. In Fig. 9, silicon-hydrogen complexes with a hydrogen molecule inside a small microvoid for models A and B are shown. The left complex and the right complex correspond to models A and B, respectively, and are surrounded by different number of hydrogen atoms. In both cases, assuming a spherical shape, the radius of the

microvoids lies within 3.0–4.0 Å. In model A, three such hydrogen pairs have been observed that are separated by a distance of 0.85–0.90 Å, whereas in model B, two molecular hydrogens have been realized. This translates into approximately 0.87–1.4% of total hydrogen atoms in models B and A, which is close to the experimental value of 0.5–1% of hydrogen as observed from nuclear magnetic resonance and calorimetric measurements. However, it should be noted that the results from the hybrid models are subject to statistical uncertainties due to the relatively small size of the models as well as the presence of very few hydrogen molecules. Thus, it is not possible to predict accurately the concentration of hydrogen molecules from this study. Nonetheless, it is evident from the present study that microvoids do exist in hydrogenated a -Si at high concentration, and that few hydrogen molecules realize inside the microvoids. This observation thus provides a direct evidence of the presence of microvoids and molecular hydrogen in a -Si:H from *ab initio* calculations guided by experimental data. Further studies with significantly larger models are needed for accurate calculation of the concentration of molecular hydrogen on a -Si:H.

VI. CONCLUSION

The distribution of hydrogen in amorphous silicon is addressed with particular emphasis on voids and molecular hydrogen at high concentration (of hydrogen) using a novel hybrid approach that directly utilizes experimental nuclear magnetic resonance data in constructing model configurations of hydrogenated amorphous silicon. Structural properties of the models are examined with particular emphasis on the two- and the three-body correlation functions.⁶⁸ The neutron-weighted total pair-correlation data for a model configuration are compared to the experimental neutron diffraction data, and are found to be in excellent agreement with the latter. Structural properties associated with the higher-order correlation functions, such as the bond-angle distributions and the co-ordination number of the atoms, are also examined for the model networks. The total bond-angle distribution and the coordination number of the atoms show that the models have the characteristic features of tetrahedral structure with an average bond angles around 108.5° and an

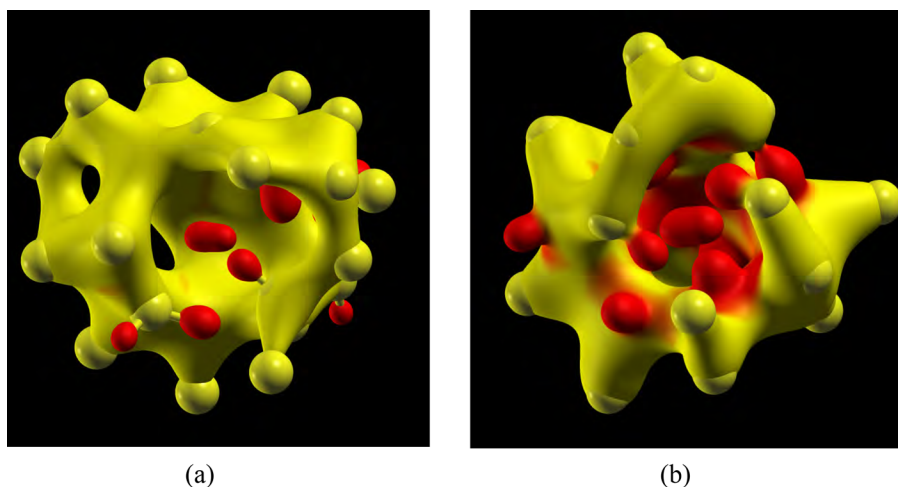


FIG. 9. Realization of a hydrogen molecule inside a void in a model of amorphous silicon. The left (model A) and the right (model B) figures show a silicon-hydrogen complex of a diameter 10 Å with the hydrogen molecule at the center of the complex.

RMS deviation near 13.3° with an average coordination number 3.99–4.003. Furthermore, the electronic density of states for the models obtained via the first-principles density functional Hamiltonian shows that the results are consistent with the conventional models of *a*-Si:H. Real space analysis of hydrogen microstructure of the model configurations in the concentration range 16–18% H shows that the distribution (of H atoms) is characterized by the presence of several hydrogen clusters with a radius of 4–6 Å in the background of a sparse or dilute distribution of H atoms with majority of the hydrogen atoms realized as monohydride (SiH) and dihydride (SiH₂) configurations. These results are in agreement with the nuclear magnetic resonance and infrared measurements as mentioned in Sec. II.

A very remarkable feature of the hybrid approach is its ability to produce small microvoids and few hydrogen molecules within the microvoids during hydrogenation that makes it possible to study structure and formation of voids in hydrogenated sample of amorphous silicon. The hydrogen microstructure of the model configurations is characterized by the presence of several microvoids and few hydrogen molecules. The microvoids have been found to be realized with a linear dimension of 3.0–4.0 Å at high concentration (>15.0% H) along with few hydrogen molecules within the voids. The shape and the size of the microvoids are highly irregular depending on the concentration of H atoms. The approximate size and the shape of the microvoids are determined by partitioning the model into small cells and constructing the Gaussian isosurfaces around the constituent atoms within the cells. This suggests that the linear size of the microvoids [within the cells] lies in the range 3.0–4.0 Å, which is equivalent to spherical voids of diameter in the range 5–7 Å. The surface of the microvoids is found to be decorated with monohydride SiH configurations, the number of which depends on the concentration and the size of the microvoids. Although the size of the models constrains us to calculate the concentration of molecular hydrogen accurately, it is noteworthy that approximately 0.9–1.4% of total hydrogen have realized in molecular state.

ACKNOWLEDGMENTS

P.B. would like to acknowledge the support from the Aubrey Keith Lucas and Ella Ginn Lucas Foundation at the University of Southern Mississippi in the form of a faculty research fellowship. D.A.D. thanks the Army Research Office for support under Award No. W911NF1110358 and the Ohio Supercomputer Center for computer time. One of us (P.B.) thanks Rajendra Timilsina for discussions.

¹D. E. Carlson and C. R. Wronski, *Appl. Phys. Lett.* **28**, 671 (1976).

²A. V. Shah, H. Schade, M. Vaneck, J. Meierl, E. Vallaut-Sauvain, N. Wyrsh, U. Kroll, C. Drozl, and J. Bailat Prog, *Photovoltaics* **12**, 113 (2004).

³B. Fieque, J. L. Tissot, C. Trouilleau, A. Crastes, and O. Legras, *Infrared Phys. Technol.* **49**, 187 (2007).

⁴K. D. Mackenzie, P. G. LeComber, and W. E. Spear, *Appl. Phys. A* **31**, 87 (1983).

⁵T. Takeda and S. Sano, *Proc. MRS Symp.* **118**, 399 (1988).

⁶A. J. Snell, K. D. Mackenzie, W. E. Spear, P. G. LeComber, and A. J. Hughes, *Appl. Phys.* **24**, 357 (1981).

⁷R. A. Street, *Hydrogenated Amorphous Silicon* (Cambridge Solid State Science Series, 1991).

⁸K. Morigaki, *Physics of Amorphous Semiconductors* (Imperial College Press, 1991).

⁹A. V. Shah, R. Platz, and H. Keppner, *Sol. Energy Mater. Sol. Cells* **38**, 501 (1995).

¹⁰T. A. Abtew, F. Inam, and D. A. Drabold, *Europhys. Lett.* **79**, 36001 (2007).

¹¹S. T. Pantelides, *Phys. Rev. Lett.* **57**, 2979 (1986).

¹²J. L. Benton, C. J. Doherty, S. D. Ferris, D. L. Flamm, L. C. Kimerling, and H. J. Leamy, *Appl. Phys. Lett.* **36**, 670 (1980).

¹³R. Bellissent, A. Menelle, W. S. Howells, A. C. Wright, T. M. Brunier, R. N. Sinclair, and F. Jansen, *Physica B* **156**, 217 (1989).

¹⁴D. L. Staebler and C. R. Wronski, *Appl. Phys. Lett.* **31**, 292 (1977).

¹⁵P. D'Antonio and J. H. Konert, *Phys. Rev. Lett.* **43**, 1161 (1979).

¹⁶W. Schüelke, *Philos. Mag.* **B 43**, 451 (1981).

¹⁷A. Filipponi, F. Evangelisti, M. Benfatto, S. Mobilio, and C. R. Natoli, *Phys. Rev. B* **40**, 9636 (1989).

¹⁸T. A. Postol, C. M. Falco, R. T. Kampwirth, I. K. Schuller, and W. B. Yelon, *Phys. Rev. Lett.* **45**, 648 (1980).

¹⁹A. C. Wright, A. C. Hannon, R. N. Sinclair, T. M. Brunier, C. A. Guy, R. J. Stewart, M. B. Strobel, and F. Jensen, *J. Phys.: Condens. Matter* **19**, 415109 (2007).

²⁰H. V. Löhneysen, J. H. Schinkand, and W. Beyer, *Phys. Rev. Lett.* **52**, 549 (1984).

²¹B. Lamotte, *Phys. Rev. Lett.* **53**, 576 (1984).

²²W. E. Carlos and P. C. Taylor, *Phys. Rev. B* **26**, 3605 (1982).

²³J. Baum, K. K. Gleason, A. Pines, A. N. Garroway, and J. A. Reimer, *Phys. Rev. Lett.* **56**, 1377 (1986).

²⁴J. A. Reimer and R. W. Vaughan, *Phys. Rev. Lett.* **44**, 193 (1980).

²⁵D. J. Leopold, J. B. Boyce, P. A. Fedders, and R. E. Norberg, *Phys. Rev. B* **26**, 6053 (1982).

²⁶C. Manfredotti, F. Fizzotti, M. Boero, P. Pastrino, P. Polesllo, and E. Vittone, *Phys. Rev. B* **50**, 18046 (1994).

²⁷K. K. Gleason, M. A. Petrich, and J. A. Reimer, *Phys. Rev. B* **36**, 3259 (1987).

²⁸S. Acco, D. L. Williamson, P. A. Stolk, F. W. Saris, M. J. van de Boogard, W. C. Sinke, W. F. van der Weg, S. Roorda, and P. C. Zalm, *Phys. Rev. B* **53**, 4415 (1996).

²⁹G. Lucovsky, R. J. Nemanich, and J. C. Knights, *Phys. Rev. B* **19**, 2064 (1979).

³⁰H. Tourier, K. Zellma, and J.-F. Morhange, *Phys. Rev. B* **59**, 10076 (1999).

³¹R. Timilsina and P. Biswas, *J. Phys.: Condens. Matter* **25**, 165801 (2013).

³²D. A. Drabold and P. A. Fedders, *Phys. Rev. B* **37**, 3440 (1988).

³³J. H. Van Vleck, *Phys. Rev.* **74**, 1168 (1948).

³⁴W. E. Carlos and P. C. Taylor, *Phys. Rev. Lett.* **45**, 358 (1980).

³⁵S. C. Moss and J. F. Graczyk, *Phys. Rev. Lett.* **23**, 1167 (1969).

³⁶M. S. Conradi and R. E. Norberg, *Phys. Rev. B* **24**, 2285 (1981).

³⁷J. E. Graebner, B. Golding, L. C. Allen, D. K. Biegelson, and M. Stutzmann, *Phys. Rev. Lett.* **52**, 553 (1984).

³⁸S. R. Elliott, *Adv. Phys.* **38**, 1–88 (1989).

³⁹J. C. Knights, in *Structural and Chemical characterization, The Physics of Hydrogenated Amorphous Silicon I, Structure, Preparation and Devices*, Springer Topics in Applied Physics Vol. 55, edited by J. D. Joannopoulos and G. Lucovsky (Springer-Verlag, Berlin, 1984), pp. 5–62.

⁴⁰P. C. Taylor, in *Magnetic Resonance Measurements in a-Si:H, Hydrogenated Amorphous Silicon, Part C, Semiconductors and Semimetals* Vol. 21, edited by J. I. Pankove (Academic, Orlando, FL, 1984), pp. 99–154.

⁴¹A. H. Mahan, D. L. Williamson, B. P. Nelson, and R. S. Crandall, *Phys. Rev. B* **40**, 12024 (1989).

⁴²D. L. Williamson, A. H. Mahan, B. P. Nelson, and R. S. Crandall, *J. Non-Cryst. Solids* **114**, 226 (1989).

⁴³A. Guinier, G. Fournet, C. B. Walker, and K. L. Yudowitch, *Small-Angle Scattering of X Rays* (Wiley, New York, 1995).

⁴⁴K. Kuglar, G. Molnar, G. Peto, E. Zsolodos, L. Rosta, A. Menelle, and R. Bellissent, *Phys. Rev. B* **40**, 8030 (1989).

⁴⁵A. H. M. Smets, W. M. M. Kessels, and M. C. M. van de Sanden, *Appl. Phys. Lett.* **82**, 1547 (2003).

⁴⁶Y. J. Chabal and C. K. N. Patel, *Phys. Rev. Lett.* **53**, 210 (1984).

⁴⁷Y. J. Chabal and C. K. N. Patel, *Rev. Mod. Phys.* **59**, 835 (1987).

⁴⁸G. E. Pake, *J. Chem. Phys.* **16**, 327 (1948).

⁴⁹J. B. Boyce and M. Stutzmann, *Phys. Rev. Lett.* **54**, 562 (1985).

- ⁵⁰B. Tuttle and J. B. Adams, *Phys. Rev. B* **53**, 16265 (1996).
- ⁵¹P. Biswas, R. Atta-Fynn, and D. A. Drabold, *Phys. Rev. B* **76**, 125210 (2007).
- ⁵²K. Jarolimek, R. A. de Groot, G. A. de Wijs, and M. Zeman, *Phys. Rev. B* **79**, 155206 (2009).
- ⁵³F. Buda, G. L. Chiarotti, R. Car, and M. Parrinello, *Phys. Rev. B* **44**, 5908 (1991).
- ⁵⁴R. Biswas, I. Kwon, A. M. Bouchard, C. M. Soukoulis, and G. S. Grest, *Phys. Rev. B* **39**, 5101 (1989).
- ⁵⁵S. Chakraborty and D. A. Drabold, *Phys. Rev. B* **79**, 115214 (2009).
- ⁵⁶D. A. Drabold, T. A. Abtey, F. Inam, and Y. Pan, *J. Non-Cryst. Solids* **354**, 2149 (2008).
- ⁵⁷S. M. Nakhmanson and D. A. Drabold, *Phys. Rev. B* **58**, 15325 (1998).
- ⁵⁸F. Wooten, K. Winer, and D. Weaire, *Phys. Rev. Lett.* **54**, 1392 (1985).
- ⁵⁹G. T. Barkema and N. Mousseau, *Phys. Rev. B* **62**, 4985 (2000).
- ⁶⁰P. Biswas, R. Atta-Fynn, and D. A. Drabold, *Phys. Rev. B* **69**, 195207 (2004).
- ⁶¹J. M. Holender and G. J. Morgan, *J. Phys.: Condens. Matter* **3**, 1947 (1991).
- ⁶²P. Klein, H. M. Urbassek, and T. Frauenheim, *Phys. Rev. B* **60**, 5478 (1999).
- ⁶³J. M. Soler, E. Artacho, J. D. Gale, A. Garcia, J. Junquera, P. Ordejon, and D. Sanchez-Portal, *J. Phys.: Condens. Matter* **14**, 2745 (2002).
- ⁶⁴J. P. Perdew and A. Zunger, *Phys. Rev. B* **23**, 5048 (1981).
- ⁶⁵N. Troullier and J. L. Martins, *Phys. Rev. B* **43**, 1993 (1991).
- ⁶⁶L. Kleinman and D. M. Bylander, *Phys. Rev. Lett.* **48**, 1425 (1982).
- ⁶⁷O. F. Sankey and D. J. Niklewski, *Phys. Rev. B* **40**, 3979 (1989).
- ⁶⁸See supplementary material at <http://dx.doi.org/10.1063/1.4905024> for the partial pair-correlation data for Si-H and H-H, and the total bond-angle distribution.
- ⁶⁹Strictly speaking, a two-body correlation function does include some characteristic features of a three-body correlation function. However, the extraction of such features from a two-body correlation function in a unique manner is highly nontrivial and, generally, requires solving an inverse problem with additional information.
- ⁷⁰The value of the bandgap in *a*-Si:H can be affected by several factors, such as the type of the basis functions, the nature of the exchange-correlation approximation, and the degree of relaxation of the model. It is not the intention of the present study to address these issues here. See Ref. **77** for a discussion.
- ⁷¹R. Timilsina and P. Biswas, *Phys. Status Solidi A* **207**, 609 (2010).
- ⁷²P. Biswas and R. Timilsina, *J. Phys.: Condens. Matter* **32**, 056801 (2011).
- ⁷³A. Kokalj, *Comput. Mater. Sci.* **28**, 155 (2003).
- ⁷⁴A. H. Mahan, D. L. Williamson, B. P. Nelson, and R. S. Crandall, *Solar Cells* **27**(1-4), 465-476 (1989).
- ⁷⁵J. A. Reimer, R. W. Vaughan, and J. C. Knights, *Phys. Rev. B* **24**, 3360 (1981).
- ⁷⁶C. G. Fry, T. M. Apple, and B. C. Gerstein, "Quantitative determination of molecular *a*-Si:H using proton NMR," Ames Laboratory-USDOE and Department of Chemistry-Iowa State University Preprint (1987).
- ⁷⁷R. Atta-Fynn, P. Biswas, P. Ordejon, and D. A. Drabold, *Phys. Rev. B* **69**, 85207 (2004).